Bioorganic Chemistry 85 (2019) 128–139

Contents lists available at ScienceDirect

Bioorganic Chemistry

journal homepage: www.elsevier.com/locate/bioorg

The first synthesis, carbonic anhydrase inhibition and anticholinergic activities of some bromophenol derivatives with S including natural products

Cetin Bayrak[a,b], Parham Taslimi[a], Halide Sedef Karaman[a], Ilhami Gulcin[a], Abdullah Menzek[a,*]

[a] Department of Chemistry, Faculty of Science, Ataturk University, 25240-Erzurum, Turkey
[b] Dogubayazit Ahmed-i Hani Vocational School, Agri Ibrahim Cecen University, 04400-Agri, Turkey

ARTICLE INFO

Keywords:
Bromination
Bromophenol
Carbonic anhydrase
Acetylcholinesterase
Enzyme inhibition
Molecular docking

ABSTRACT

Starting from vanillin, known four benzyl bromides with Br were synthesized. The first synthesis of natural product 3,4-dibromo-5-((methylsulfonyl)methyl)benzene-1,2-diol (**2**) and 3,4,6-tribromo-5-((methylsulfonyl) methyl)benzene-1,2-diol (**3**) and derivatives were carried out by demethylation, acetylatilation, oxidation and hydrolysis reactions of the benzyl bromides. Also, these compounds were tested against some important enzymes like acetylcholinesterase and butyrylcholinesterase enzymes, carbonic anhydrase I, and II isoenzymes. The novel bromophenols showed Ki values of in range of 53.75 ± 12.54–234.68 ± 46.76 nM against hCA I, 42.84 ± 9.36 and 200.54 ± 57.25 nM against hCA II, 0.84 ± 0.12–14.63 ± 3.06 nM against AChE and 0.93 ± 0.20–18.53 ± 5.06 nM against BChE. Induced fit docking process performed on the compounds inhibiting hCA I, hCA II, AChE, and BChE receptors. Hydroxyl group should exist at the aromatic ring of the compounds for inhibition of the enzymes. The moieties reported in this study will be useful for design of more potent and selective inhibitors against the enzymes.

1. Introduction

It is known that various bromophenols are often isolated from red algae of the family *Rhodomelaceae* in marine life [1]. Important biological activities such as antioxidant [1,2] and feeding deterrent effects [3] of the bromophenols were reported. We investigated the carbonic anhydrase (CA), [4] acetylcholinesterase (AChE) and butyrylcholinesterase (BChE) [5] and paraxonase [6] inhibitory properties of bromophenol derivatives.

As seen Fig. 1, 5-(methoxymethyl)-4-((methylsulfonyl)methyl)benzene-1,2,3-triol (**1**), 3,4-dibromo-5-((methylsulfonyl)methyl)benzene-1,2-diol (**2**) and 3,4,6-tribromo-5-((methylsulfonyl)methyl)benzene-1,2-diol (**3**) are compounds having methylsulfonyl group. These phenol derivatives **1–3**, natural product, were isolated from the marine alga *Grateloupia filicina* (Wulfen), [7] marine red alga *Rhodomela confervoides* [2c] and marine red alga *Symphyocladia latiuscula* [2a], respectively. Natural bromophenols **2** and **3** exhibit antioxidant activities [2a,c].

The interconversion amongst HCO_3^- and CO_2 is an essential mechanism for the significant flow of biochemical mechanisms in all-living body cells. The metabolic transformation is performed by the hydration of carbon dioxide, that gives rise to the corresponding bicarbonate, soluble ion, and the emancipation of a proton [8]. CA isoenzymes are metalloenzymes that catalyse the reversible act of CO_2 into protons and bicarbonate and hence are necessary for maintaining extracellular and intracellular pH [9]. CA isoforms are discovered in all three domains of life and these enzymes belong to diverse families: α-, β-, γ-, δ-, ζ-, η- and θ-CAs. α-CA isozymes exist in many organisms, such as fungi cells (together with β-CAs) [10]. β-CA isozymes are also found in archaea, plants, and both prokaryotes and eukaryotes [11]. γ-CA isozymes are found in bacteria cells. ζ-CAs and δ-CA isoforms exist in some marine planktonic kinds [12]. η-CAs and θ-CAs are found in malaria causative agent, *Plasmodium falciparum*, and in marine diatom *Phaeodactylum tricornutum*, respectively [13]. CA isoforms have Zn^{2+} ions in their active centre, although certain can have cobalt, cadmium, and iron ions. Human cells have sixteen α-CA isozymes but only 12 of them possess Zn^{2+} ion and are catalytically active. Human CAs belongs to the α-CA family and are Zn^{2+} containing metalloenzymes [14].

Alzheimer's disease (AD) is an advanced neurodegenerative pathology disorder with social impact and intense economic [15]. Nowadays, drug development and research are based on the cholinergic hypothesis which proposes the elective harm of cholinergic neuron cells

* Corresponding author.
E-mail address: amenzek@atauni.edu.tr (A. Menzek).

https://doi.org/10.1016/j.bioorg.2018.12.012
Received 11 September 2018; Received in revised form 4 December 2018; Accepted 10 December 2018
Available online 14 December 2018

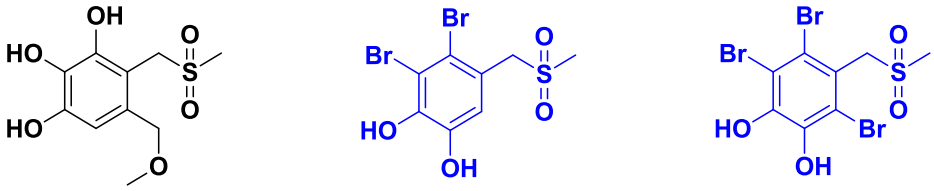

Fig. 1. Natural phenol compounds having methylsulfonyl group.

outcomes in a deficiency of acetylcholine (ACh) in special areas of the brain that mediate memory functions and learning [16]. Presently accessible therapy for patients suffering from AD involve approved AChE inhibitors such as donepezil, rivastigmine, and galantamine, which avoid the hydrolysis of ACh therewith raising its concentrations [17]. Levels of AChE and BChE manifestly show that these enzymes play a key role in disease manifestation and progression. Some other studies have pointed to the significant role of AChE enzyme in the promotion of Aβ oligomerization. Accordingly, the administration of AChE and BChE inhibitors is most clinically related palliative strategy for decreasing AD symptoms, while another therapy strategy is failing [18].

To the best of our knowledge, bromophenols **2** and **3**, biologically active natural products have not yet been synthesized. In addition to these, no biological activity was investigated except for the antioxidant activity of the bromophenols **2** and **3**. In the present study, we report the first synthesis of these natural products **2**, **3** and their derivatives and their hCA I, hCA II, AChE and BChE inhibitory properties.

2. Results and discussion

2.1. Chemistry

Biologically active natural bromophenols **2** and **3** include methylsufonyl and benzyl whose aromatic ring are highly brominated groups (Fig. 1). Synthesis of benzyl(methyl)sulfane from reaction of benzyl bromide with NaSMe at mild condition is known [19]. Oxidation of sulfanes with meta-choloroperbenzoic acid (m-CPBA) to sulfanes is also knonw [20]. For the synthesis of these bromophenols and their derivatives, favorite method is as follows: (i) preparing benzyl bromides such as **4** and **5** starting with vanillin; (ii) substitutions of the benzyl bromides with NaSMe; (iii) oxidation and demethylation of the corresponding benzyl(methyl)sulfanes.

After benzyl bromides **4–7** were synthesized by known method, [5a,21] and reactions of them with NaSMe at room temperature (RT) for 24 h gave corresponding benzyl(methyl)sulfanes **8–11** in high yields (Scheme 1). By oxidation of the compound **8** with m-CPBA, sulfone **12** was obtained and then its reaction with BBr_3 did not give natural bromophenol **3** (Scheme 1).

As another way for the synthesis of the natural bromophenols and their derivatives, demethylations, [4,5,22] acetylations [23] and hydrolysis of the benzyl(methyl)sulfanes **8–11** were thought, respectively. After demethylation of the benzyl(methyl)sulfanes **8–11** with BBr_3 in CH_2Cl_2 were performed, and then diols which were formed in situ were reacted with Ac_2O (acetic acid anhydride) (Scheme 2). Sulfanes with diacetates **13–16** were synthesized from these reactions. There are characteristic peaks (as singlet) belonging OMe and Me (in acetates) of products in their NMR spectra. From these peaks, peaks of OMe in **8–11** and Me in **13–16** were observed in their NMR spectra. Also, all data of them consist with the proposed structures.

Oxidation of the diacetates **13–16** with m-CPBA at RT gave their sulfones **17–20** (Scheme 2). In the compounds, SO_2 are more electron-withdrawing group than S. As expected, the chemical shifts of the hydrogens (CH_2 and CH_3) in the adjacent carbon atoms of sulfur atom in **17–20** are lower field than those of sulfur atom in **13–16**. These chemical shifts for CH_2 and CH_3 are 3.61–4.23 ppm and 1.98–2.21 ppm for **13–16** and 4.18–4.96 ppm and 2.82–2.96 ppm for **17–20**, respectively.

To synthesize the natural bromophenols **2** and **3**, diacetates groups in **17** and **18** should be hydrolyzed because the OAc also is a protecting group of OH group. Hydrolysis of these groups with H_2SO_4/MeOH at reflux temperature gave natural bromophenol **2** and **3** in high yields. Also, bromophenols **21** and **22** were obtained from **19** and **20** by similar reactions. Synthesis of bromophenols **2**, **3**, **21** and **22** in this work are the first synthesis of them (Scheme 2).

3. Biological activities

Since unusual amounts or activities of most sixteen hCA isoenzymes have been frequently associated with various human diseases, these isoforms have raised an intense interest for the synthesis and design of inhibitor compounds which selectively purpose special isoenzymes, in order to decrease the overall side efficacy elicited by most non-isoform elective CAIs clinically utilized up to now [24]. These isoforms are

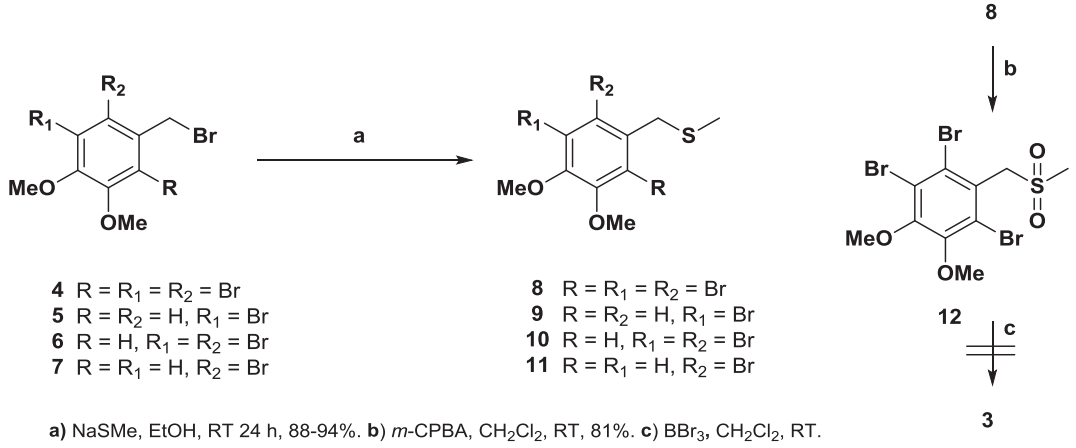

a) NaSMe, EtOH, RT 24 h, 88-94%. **b**) *m*-CPBA, CH_2Cl_2, RT, 81%. **c**) BBr_3, CH_2Cl_2, RT.

Scheme 1. Synthesis of benzyl(methyl)sulfanes **8–11** and attempt to obtain natural bromophenol **3** from sulfone **12**.

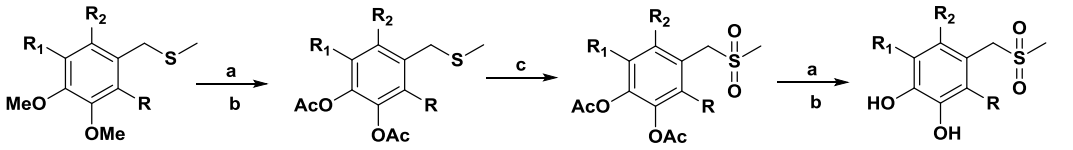

8 R = R_1 = R_2 = Br
9 R = R_2 = H, R_1 = Br
10 R = H, R_1 = R_2 = Br
11 R = R_1 = H, R_2 = Br

13 R = R_1 = R_2 = Br
14 R = R_2 = H, R_1 = Br
15 R = H, R_1 = R_2 = Br
16 R = R_1 = H, R_2 = Br

17 R = R_1 = R_2 = Br
18 R = R_2 = H, R_1 = Br
19 R = H, R_1 = R_2 = Br
20 R = R_1 = H, R_2 = Br

2 R_1 = R_2 = Br, R = H
3 R = R_1 = R_2 = Br
21 R_1 = Br, R = R_2 = H
22 R = R_1 = H, R_2 = Br

a) BBr_3, CH_2Cl_2 0 - 25°C **b)** NEt_3 / Ac_2O, CH_2Cl_2, RT, 24 h, 83-92%. **c)** *m*-CPBA, CH_2Cl_2, RT, 24 h, 76-84%.
c) H_2SO_4 / MeOH, Reflux, 6 h, 83-92%.

Scheme 2. Bromophenols including (methylsulfonyl)methyl group **2**, **3**, **21** and **22** from starting material bromophenol derivatives with (methylthio)methyl group **8–11**.

extensively distributed in diverse organs and tissues, where these isoforms are involved in many crucial physiological mechanisms like CO_2 and pH homeostasis, proliferation and cell differentiation, bone calcification/resorption, electrolyte secretion, neurotransmission in mammals, gluconeogenesis, and tissue and virulence colonization (in diverse pathogens, like protozoa, bacteria, and fungi [25]. Thus, many CA isoforms are noteworthy aims for many pharmacological applications like diuretics, antiglaucoma drugs, antiobesity, antitumor and anticonvulsant factors/diagnostic tools. For instance, inhibitors targeting hCA I are involved in cerebral edema and retinal, inhibitor compounds targeting hCA II, IV, XII and XIV are utilized in the management edema, antiepileptic drugs, as diuretics and antiglaucoma agents, and also for the therapy of altitude sickness [26] Recently, the inhibitors of the hCA IX and XII isoforms have recorded applications as diagnostic factors for imaging hypoxic tumors and as antimetastatic/antitumor factors [27].

For hCA I isoform, the Ki values were determined in range of 53.75 ± 12.54–234.68 ± 46.76 nM. In comparison, the Ki for the standard CA inhibitor AZA, a definitive hCA I inhibitor, was 273.61 ± 76.86 nmol against hCA I (Table 1). All novel benzyl(methyl)sulfane derivative bromophenols (**2**, **3**, **8–11**, **13–22**) had effective inhibition effects than that of AZA. Also, between these compounds, novel natural product 3-bromo-5-((methylsulfonyl)methyl)benzene-1,2-diol (**21**), which had two hydroxyl groups (−OH) and two bromine group (−Br), was the best hCA I inhibitor (Ki 53.75 ± 12.54 nM). It is well known that molecules containing halogen and carbonyl (−CO) groups are effective CA inhibitors. The hCA I isoform is discovered in many mammalian tissues and happens in high concentrations in the gastrointestinal tract and blood cells [28]. It is involved in cerebral edema and retinal, and also the inhibition of this enzyme can be an important factor for fighting these situations or diseases. As shown in Table 1, IC_{50} values are in the range of 58.16–204.72 nM towards cytosolic hCA I isoenzyme, and in the range of 45.04–184.02 nM for hCA II isoenzyme.

Novel benzyl(methyl)sulfane derivative bromophenols (**2**, **3**, **8–11** and **13–22**) synthesized in this paper significantly inhibited hCA II with Ki in the low nanomolar range. Ki values were calculated between 42.84 ± 9.36 and 200.54 ± 57.25 nM (Table 1 and Fig. 2). On the other hand, novel natural product 3-bromo-5-((methylsulfonyl)methyl) benzene-1,2-diol (**21**), which had two hydroxyl groups (−OH) and two bromine group (−Br), is in fact the best inhibitor in this molecules, being 5.34 times a better hCA II inhibitor compared to the clinical candidate drug (Ki of AZA: 229.08 ± 55.14 nM). The hCA II has key role in diseases such as glaucoma disease. Indeed, HCO_3^- generation serves as a strategy to transport sodium ions (Na^+) into the eye along with the influx of water leading to an increase in intraocular pressure [29]. Thus, hCA II inhibition reduces HCO_3^- production and finally aqueous humor secretion, which leads to reduced pressure in the eye. These bromophenols are also an effective hCA II inhibitor, being almost 3 times more effective than AZA in inhibiting hCA II isoform.

AChE is a fundamental enzyme that catalyzes the breakdown of ACh

Table 1
Human carbonic anhydrase I, and II (hCA I, and II) isoenzymes, acetylcholinesterase (AChE), and butyrylcholinesterase (BChE) enzymes inhibition effects of novel benzyl(methyl)sulfane derivative bromophenols (**2, 3, 8–11** and **13–22**).

Compounds	IC_{50} (nM)								K_i (nM)				
	hCA I	r^2	hCA II	r^2	AChE	r^2	BChE	r^2	hCA I	hCA II	AChE	BChE	AChE/BChE
2	83.04	0.9734	58.34	0.9812	2.04	0.9714	1.84	0.9683	89.37 ± 11.45	67.05 ± 14.73	1.53 ± 0.23	0.93 ± 0.20	1.64
3	69.35	0.9804	50.44	0.9526	1.63	0.9893	8.14	0.9937	64.12 ± 15.18	54.76 ± 8.04	0.84 ± 0.12	3.73 ± 1.03	0.22
8	105.83	0.9632	83.18	0.9495	8.24	0.9345	14.05	0.9487	116.07 ± 35.88	94.03 ± 26.47	5.64 ± 1.04	11.54 ± 1.88	0.48
9	137.18	0.9738	118.34	0.9975	9.31	0.9811	14.95	0.9940	157.13 ± 29.76	105.63 ± 24.74	6.33 ± 2.01	10.40 ± 2.43	0.60
10	123.63	0.9881	104.83	0.9729	5.12	0.9730	6.04	0.9374	146.11 ± 30.55	117.04 ± 21.62	2.74 ± 0.90	4.26 ± 0.93	0.64
11	109.62	0.9748	102.07	0.9803	2.04	0.9872	9.63	0.9798	103.67 ± 25.13	100.52 ± 17.38	1.99 ± 0.18	5.95 ± 1.04	0.33
13	174.43	0.9682	134.88	0.9645	13.84	0.9937	20.64	0.9307	208.26 ± 43.76	167.46 ± 43.67	9.02 ± 1.05	13.65 ± 2.64	1.51
14	98.63	0.9744	91.84	0.9893	6.53	0.9457	8.02	0.9748	111.43 ± 17.37	98.64 ± 14.86	4.52 ± 1.01	5.94 ± 0.99	0.76
15	173.84	0.9814	167.23	0.9574	13.10	0.9915	11.53	0.9902	186.36 ± 76.23	154.83 ± 30.57	10.64 ± 2.64	7.91 ± 1.76	1.34
16	204.72	0.9602	184.02	0.9830	10.62	0.9693	10.77	0.9711	234.68 ± 46.76	200.54 ± 57.25	7.43 ± 1.54	8.64 ± 1.55	0.86
17	148.93	0.9034	121.33	0.9599	7.14	0.9485	8.63	0.9837	168.34 ± 28.09	115.85 ± 16.04	5.24 ± 0.95	6.53 ± 0.93	0.80
18	111.53	0.9738	100.62	0.9934	5.03	0.9384	9.39	0.9928	103.64 ± 20.64	94.83 ± 11.65	3.58 ± 0.86	6.63 ± 1.88	0.54
19	150.28	0.9836	128.38	0.9655	12.22	0.9476	11.03	0.9475	147.04 ± 35.85	137.45 ± 25.76	8.54 ± 1.76	8.35 ± 1.40	1.02
20	137.05	0.9508	108.64	0.9937	18.04	0.9845	25.17	0.9742	148.34 ± 54.76	119.46 ± 24.78	14.63 ± 3.06	18.53 ± 5.06	0.78
21	58.16	0.9712	45.04	0.9749	2.74	0.9663	3.73	0.9205	53.75 ± 12.54	42.84 ± 9.36	1.05 ± 0.32	2.04 ± 0.63	0.51
22	61.73	0.9814	50.02	0.9727	3.08	0.9305	4.18	0.9848	57.43 ± 10.16	53.75 ± 12.58	1.32 ± 0.43	2.75 ± 0.84	0.48
AZA*	265.41	0.9954	248.54	0.9714	–	–	–	–	273.61 ± 76.86	229.08 ± 55.14	–	–	–
TAC$^{\Psi}$	–	–	–	–	32.20	0.9796	40.16	0.9711	–	–	16.37 ± 5.10	23.40 ± 3.62	0.70

* Acetazolamide (AZA) was used as a standard inhibitor for both carbonic anhydrases I, and II (hCA I and II) isoenzymes.
$^{\Psi}$ Tacrine (TAC) was used as a standard inhibitor for acetylcholinesterase (AChE), and butyrylcholinesterase (BChE) enzymes.

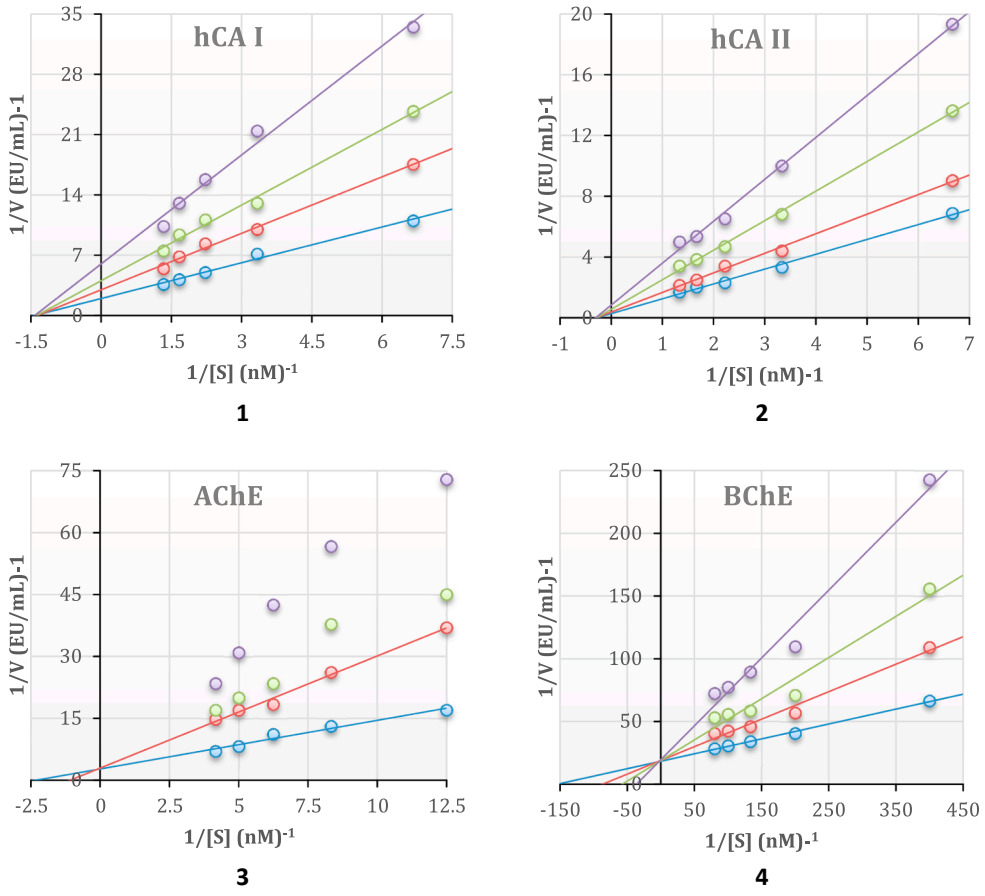

Fig. 2. Determination of Lineweaver-Burk graphs for excellent inhibitors of hCA I and II (**21**), AChE (3), and BChE (**2**) compounds.

and some other choline ester molecules that used as neurotransmitter factors, which are recorded as drug aims for AD [30]. The cholinergic hypothesis was first proposed to describe AD and was based on the finding that the synaptic depression is hindered due to the prevention of the ACh hydrolysis in the cholinergic neuron cells [31]. The inhibition of AChE results in the obstruction of ACh hydrolysis. Thus, the design of inhibitor compounds and/or modulator for AChE enzyme is of Intense interests since it is presently one of the most significant aims to prevent AD, resulting in three commercial drugs recorded by FDA like galantamine, donepezil, rivastigmine and tacrine [32]. Some of compounds are under clinical evaluation like huperzine A and ganstigmine [33]. The Ki values of novel benzyl(methyl)sulfane derivative bromophenols (**2**, **3**, **8–11**, **13–22**) for BChE and AChE were obtained from Lineweaver-Burk plots. Also, tacrine, which was the first cholinesterase inhibitor to be discovered for the management of AD symptoms in 1993, had Ki value of 100.40 ± 15.62 nM. Furthermore, it was considered that donepezil hydrochloride, which is used for the therapy of mild-to-moderate AD and diverse other memory impairments, had been shown to lower AChE inhibition activity (IC_{50}: 55.0 nM). As seen in Table 1, IC_{50} values are in the range of 1.63–18.04 nM towards AChE, and 1.84–25.17 nM towards BChE. In this work, AChE was also extremely inhibited by novel benzyl(methyl)sulfane derivative bromophenols (**2**, **3**, **8–11** and **13–22**) at the low nanomolar inhibition with Ki values in range of 0.84 ± 0.12–14.63 ± 3.06 nM (Table 1). These results nicely determined that newly synthesized bromophenols had effective AChE inhibition properties. However, the most powerful AChE inhibition was recorded by novel natural product 3,4,6-tribromo-5-((methylsulfonyl)methyl)benzene-1,2-diol (**3**), which had two hydroxyl groups (−OH) and three bromine group (−Br) with a Ki value of 0.84 ± 0.12 nM. All the remaining newly these compounds reported here were highly efficient inhibition constants against AChE. Recently, evaluation of the crystallographic structures of AChE enzyme and its complex with inhibitor compounds has provided information regarding the pharmacophoric features necessary to key interactions and to elucidate the underlying catalytic mechanism for the discovery of new and powerful AChEIs [34]. Additionally, tacrine (1,2,3,4-tetrahydroacridin-9-amine), which first centrally acting cholinesterase inhibitor recorded for the therapy of AD obtained with Ki value of 16.37 ± 5.10 nM against cholinergic AChE. Finally, novel benzyl(methyl)sulfane derivative bromophenols (**2**, **3**, **8–11**, **13–22**) inhibited BChE with Ki values in range of 0.93 ± 0.20–18.53 ± 5.06 nM (Table 1, Fig. 2). However, the most powerful BChE inhibition was recorded by novel natural product 3,4-dibromo-5-((methylsulfonyl)methyl)benzene-1,2-diol (**2**), which had two hydroxyl groups (−OH) and one bromine group (−Br) with a Ki value of 0.93 ± 0.20 nM.

3.1. *In silico studies*

The ADME analyses of the most active compounds were performed by comprising to properties of a particular molecule with those of 95% of known drugs using QikProp module. Results of ADME analyses were used to classify the compounds according to physically significant descriptors and pharmaceutically relevant properties of the compounds. In order to screening potential drug candidates, the properties referred to drug-likeness were used. The ADME properties of the compounds are demonstrated in Table 2. The properties of the compounds were examined whether they are eligible with those of commercial drugs, in the light of Lipinski's rule of five. All most active compounds have less molecular weight than 500D. All most active compounds have 2 hydrogen bond acceptors (AHB) and 5.5 hydrogen bond donors (DHB). Octanol/water partition coefficients of the compounds are acceptable ranges in light Lipinski's rule. The compounds exhibited noteworthy

Table 2
Physically and pharmaceutically properties of the most active compounds.

Compound	[a]MW	[b]DHB	[c]AHB	[d]logPo/w	[e]logHERG	[f]logBB	[g]MDCK	[h]logKhsa	[i]% Hum. Oral Abs.
2	360.017	2	5.5	0.988	−3.682	−0.769	571.517	−0.499	76.903
3	438.913	2	5.5	1.490	−3.551	−0.503	1585.065	−0.414	82.390
21	281.121	2	5.5	0.598	−3.729	−0.919	287.941	−0.575	73.612

[a] Molecular weight.
[b] Number of hydrogen bond donors.
[c] Number of hydrogen bond acceptors.
[d] Octanol/water partition coefficient.
[e] IC_{50} value for blockage of HERG K^+ channels.
[f] B/blood partition coefficient.
[g] Cell permeability in nm/s.
[h] Binding to human serum albumin.
[i] Qualitative human oral absorption.

Table 3
IFD Glide scores (kcal/mol) of the most active compounds in the catalytic sites of hCA I, and hCA II, AChE, and BChE.

Compounds	IFD Glide Score			
	hCA I	hCA II	AChE	BChE
2	–	–	–	−6.625
3	–	–	−7.500	–
21	−8.528	−8.830	–	–
AZA*	−9.016	−9.560	–	–
TAC**	–	–	−9.579	−8.830

* Acetazolamide (AZA) was used as a standard inhibitor for human carbonic anhydrase isoenzymes I, and II (hCA I, and II).
** Tacrine (TAC) was used as a standard inhibitor for acetylcholinesterase (AChE) and butyrylcholinesterase (BChE) enzymes.

range IC_{50} value for HERG K^+ channel blockage (logHERG) at values above −5 and range brain/blood partition coefficient (logBB). Human oral absorption percentage of most active compounds is in appropriate ranges. The MDCK epithelial cell lines are commonly used as a possible tool for assessing the membrane permeability properties. PMDCK value of drugs should be high than 500 for great membrane permeability. We think that compounds **2** and **3** from most active compounds possess great membrane permeability with value higher than 500, however membrane permeability of c **21** doesn't look good enough. ADME analyses result clearly demonstrated that physicochemical and pharmacokinetic properties of the most active compounds are compatible with Lipinski's rule [35] (see Table 3).

3.2. Catalytic active site

We have used SiteMap to explore the catalytic site on the receptors. The most important property calculated by SiteMap is an overall SiteScore, which has proven to be effective at identifying known catalytic sites in co-crystallized complexes. SiteScores of binding sites were calculated as 1.063, 0.971, 1.090, and 1.150 for hCA I, hCA II, AChE, and BChE, respectively. The other important property calculated by SiteMap is Dscore which has indicated whether the catalytic site can be druggable or not. Dscores of the binding sites were calculated as 1.061, 0.945, 1.113, and 1.217 for hCA I, hCA II, AChE, and BChE, respectively. SiteMap results indicated that identified binding sites have catalytic sites properties due to their SiteScores and are druggable sites due to their Dscore. Moreover, we have presented ligand bonded catalytic sites surface including hydrophilic, hydrophobic, and metal binding sites in Fig. 3.

3.3. Molecular docking

The most active compounds were docked into catalytic active site of hCA I, hCA II, AChE, and BChE receptors by IFD protocol which provide flexibility both ligand and receptor. We firstly tested reliability of the IFD protocol by re-docking inhibitor complexed into the crystal structure of the receptors. IFD results were analyzed in the perspective of ligand-binding pose. The results have shown that co-crystallized and docked ligands were located in very similar region of the receptors as seen in Fig. 4. After IFD protocol validation, we analyzed IFD results of most active compounds with regard to binding energies of ligand-receptor complex, interactions between ligand and receptor, efficiency of ligand-binding site, and ligand-binding pose (see Fig. 5).

Superimposed pose and detailed binding mode of the most active compounds were shown in Fig. 6. The compounds fit into the catalytic active site of the receptors. 3-Bromobenzene-1,2-diol moiety of the compound **21** was closely surrounded by metal binding site residue including Zn301 and hydrophilic residues including Gly92, His94, and His96 and methylsulfonyl oxygen moiety was also closely surrounded by hydrophilic Gly92 residue in catalytic active site of hCA I as seen in Fig. 3a and 6a. The moieties of compound **21** were surrounded by almost similar residues in catalytic active site of hCA II as seen in Figs. 3b and 6b. Almost all of 3,4,6-tribromo benzene-1,2-diol and methylsulfonyl moieties of the compound **3** were surrounded by hydrophobic residues including Tyr72, Tyr124, Trp286, Leu289, Val294, Phe295, Phe297, Tyr337, Phe338, and Tyr341 residues in catalytic active site of AChE as seen in Figs. 3c and 6c. While 3,4-dibromo benzene-1,2-diol moiety of the compound **2** was closely surrounded by both hydrophilic residues including Glu197 and Ser198 and hydrophobic Trp82 residue, methylsulfonyl moiety of the compound was closely surrounded by hydrophobic residues including Met437 and Tyr440 as seen in Figs. 3d and 6d.

In conclusion, Starting from vanillin, the known [5a,10] benzyl bromides **4–7** were obtained and reactions of them with NaSMe gave the corresponding substitution products **8–11**. The sulfone **12** was synthesized from the oxidation of substitution product **8** with m-CPBA, and its reaction with BBr_3 did not give natural bromophenol **3**. Demethylation with BBr_3, acetylation with Ac_2O, oxidation with m-CPBA and hydrolization with acid of the substitution products **8–11** were performed, respectively. The first synthesis of the new bromophenols **2**, **3**, **21** and **22** were realized from these reactions. Two of the bromophenols are natural products **2** and **3**. Additionally, the novel molecules were investigated for BChE, AChE, hCA I, and hCA II enzymes inhibition effects. As we explained above, novel benzyl(methyl)sulfane derivative bromophenols (**2**, **3**, **8–11** and **13–22**) can be good candidate drugs, the same as AChE, BChE, and carbonic anhydrase inhibitor compounds, for therapy of some diseases like AD, epilepsy, glaucoma, gastric and duodenal ulcers, mountain sickness, osteoporosis or neurological disorders. The binding affinities and interactions of the most active compounds have provided more insight into the mode of binding of the compounds into the receptors. Hydroxyl group on bromophenol moiety of the compounds is crucial for inhibition of hCA I, hCA II,

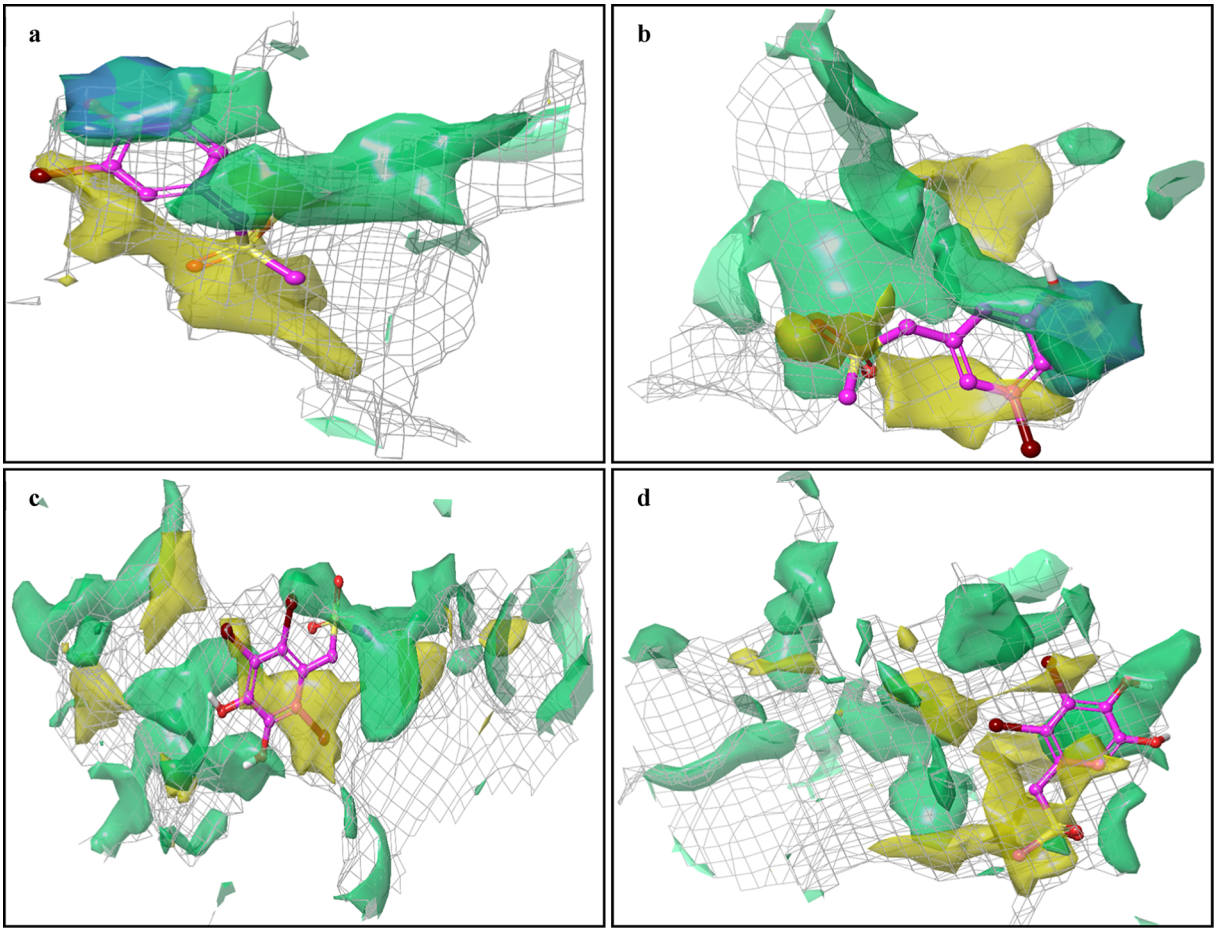

Fig. 3. Results of SiteMap analyses. (a) 21-hCA I, (b) 21-hCA II, (c) 3-AChE, and (d) 2-BChE. Binding site is represented as grey mesh, hydrophilic site is represented as green surface, hydrophobic site is represented as yellow surface, and metal binding site is represented as blue surface.

AChE, and BChE receptors. Moreover, oxygen on methylsulfonyl moiety promotes inhibition of particularly hCA II and AChE receptors.

4. Experimental section

4.1. General experimental procedures

Solvents were purified and dried by known methods. For all compounds, values as well as Mp, IR Spectra, ^{1}H and ^{13}C NMR spectra, chemical shift, elemental analyses, and CA inhibitory properties of samples were performed as explained previously [5a,36]. PLC (preparative thick-layer chromatography) was used as 1 mm of silica gel 60 PF (Merck, Darmstadt, Germany) on glass plates. HRMS data were obtained by LC-MS-TOF electrospray ionization technique (1200/6210, Agilent). The benzyl bromides **4**–**7** used in the reactions were synthesized by known ways [5a,21].

4.2. Synthesis

4.2.1. Synthesis of methyl(2,3,6-tribromo-4,5-dimethoxybenzyl)sulfane (8), standard procedure for substitution reaction with NaSMe

To solution of the bromide **4** (0.4 g, 855.11 μmol) in EtOH (50 mL) was added NaSMe (62.93 mg, 897.86 μmol), and reaction mixture was stirred at RT for 24 h. After the solvent was removed under vacuum and water (2 mL) was added, the mixture was neutralized by cold solution of HCl (%1) and extracted with CH_2CI_2 (2 × 20 mL). Combined extracts were dried over Na_2SO_4 and the solvent was evaporated removed under vacuum. The sulfane **8** (1.044 g, 90%) as a white solid. M.p = 30–32 °C; ^{1}H NMR (400 MHz, $CDCl_3$): 4.22 (s, CH_2S, 2H), 3.90 (s, 2× OMe, 6H), 2.22 (s, CH_3S 3H); ^{13}C NMR (100 MHz, $CDCl_3$): 150.96 (C), 150.75 (C), 135.90 (C), 122.49 (C), 121.91 (C), 120.40 (C), 60.88 (OMe), 60.82 (OMe), 40.94 (CH_2S), 16.16 (CH_3S); IR (CH_2Cl_2, Vmax cm^{-1}): 2935, 1452, 1393, 1366, 1278, 1051, 1010; Rf = 0.59 EtOAc/hexane (5:95); HRMS (APCI – TOF) (*m/z*) calcd for $C_{10}H_{11}{}^{79}Br_3O_2S$: 431.8030; found: 431.8037.

4.2.2. Synthesis of (3-bromo-4,5-dimethoxybenzyl)(methyl)sulfane (9)

This reaction was performed according to the standard procedure described in Section 4.2.1. In the reaction, bromide **5** (0.5 g, 1.61 mmol), EtOH (40 mL) and NaSMe (124.35 mg, 1.77 mmol) were used. The sulfane **9** (0.4 g, 90%) was obtained as a yellow liquid; ^{1}H NMR (400 MHz, $CDCl_3$): 7.05 (bs, aromatic 1H), 6.84 (d, aromatic, 1H), 3.87 (s, OCH_3, 3H), 3.84 (s, OCH_3, 3H), 3.59 (s, CH_2, 2H), 2.01 (s, CH_3, 3H); ^{13}C NMR (100 MHz, $CDCl_3$): 153.69 (C), 145.46 (C), 135.44 (C), 124.83 (CH), 117.26 (C), 112.15 (CH), 60.54 (OMe), 56.09 (OMe), 37.90 (CH_2S), 15.06 (CH_3); IR (CH_2Cl_2, v_{max} cm^{-1}): 2915, 1595, 1567, 1489, 1411, 1274, 1139, 1047; R_f = 0.40 EtOAc/hexane (5:95); HRMS (APCI-TOF) (*m/z*) calcd for $C_{10}H_{13}{}^{79}BrO_2S$: 275.9820; found: 275.9806.

4.2.3. Synthesis of (2,3-dibromo-4,5-dimethoxybenzyl)(methyl)sulfane (10)

This reaction was performed according to the standard procedure described in Section 4.2.1. In the reaction, bromide **6** (0.30 g, 771.44 μmol), EtOH (40 mL) and NaSMe (59.47 mg, 848.59 μmol) were used. The sulfane **10** (0.40 g, 90%) was obtained as a brown liquid; ^{1}H NMR (400 MHz, $CDCl_3$): 6.88 (s, aromatic, 1H), 3.80 (s, OMe, 3H), 3.76 (s, CH_2, 2H), 3.75 (s, OMe, 3H), 2.00 (s, CH_3, 3H); ^{13}C NMR (100 MHz,

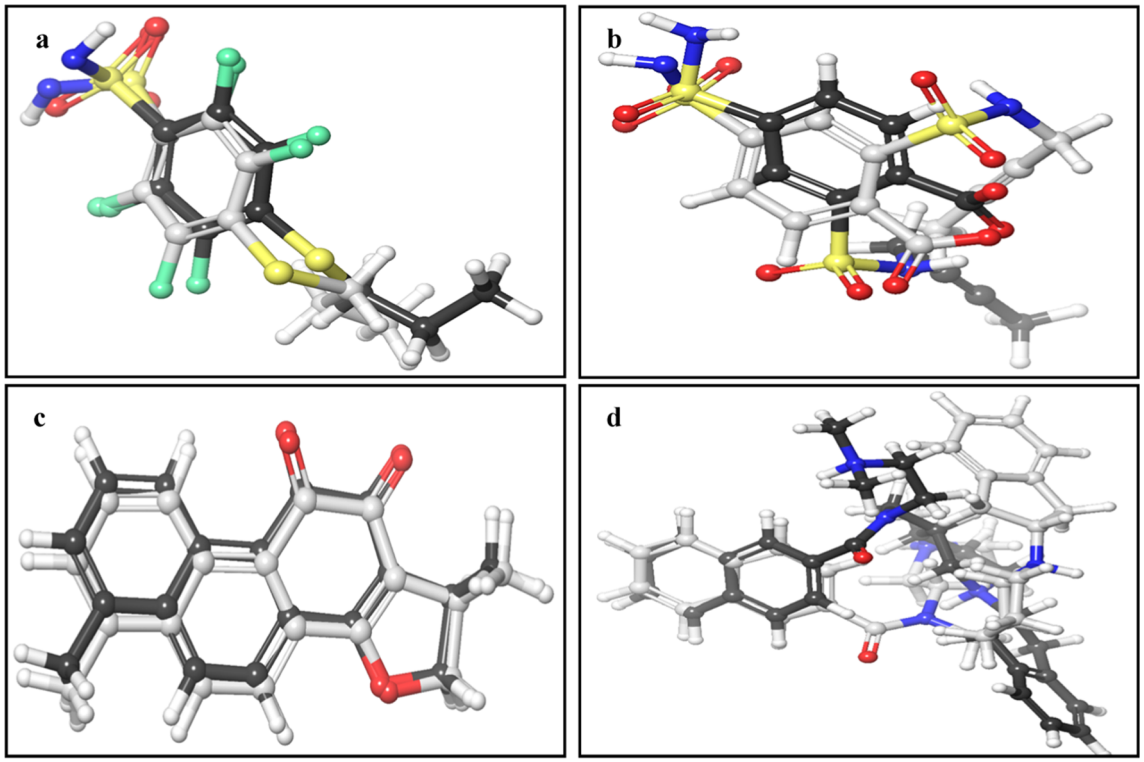

Fig. 4. Docking validation. (a) 21-hCA I, (b) 21-hCA II, (c) 3-AChE, and (d) 2-BChE. The poses of co-crystallized ligands are represented in black color ball and stick modeling while that of docked ligands is represented in grey color ball and stick mode.

$CDCl_3$): 152.40 (C), 146.61 (C), 135.05 (C), 122.08 (C), 117.66 (C), 113.27 (CH), 60.51 (OMe), 56.25 (OMe), 40.23 (CH_2S), 15.43 (CH_3S); IR (CH_2Cl_2, v_{max} cm^{-1}): 2917, 2848, 1582, 1548, 1469, 1422, 1372, 1372, 1308, 1263, 1059; R_f = 0.37 EtOAc/hexane (5:95); HRMS (APCI-TOF) (*m/z*) calcd for $C_{10}H_{12}{}^{79}Br_2O_2S$: 353.8925; found: 353.8918.

4.2.4. *Synthesis of 2-bromo-4,5-dimethoxybenzyl)(methyl)sulfane (**11**)*

This reaction was performed according to the standard procedure described in Section 4.2.1. In the reaction, bromide **7** (1.0 g, 3.23 mmol), EtOH (40 mL) and NaSMe (248.70 mg, 3.55 mmol) were used. The sulfane **11** (0.79 g, 88%) was obtained as a yellow liquid; ^1H NMR (400 MHz, $CDCl_3$): 7.00 (s, aromatic, 1H), 6.90 (s, aromatic, 1H), 3.86 (s, OMe, 3H), 3.84 (s, OMe, 3H), 3.75 (s, CH_2, 2H), 2.05 (s, CH_3, 3H); ^{13}C NMR (100 MHz, $CDCl_3$): 148.59 (C), 148.45 (C), 129.52 (C), 115.50 (CH), 114.40 (C), 113.26 (CH), 56.13 (OMe), 56.05 (OMe). 37.90 (CH_2), 15.02 (CH_3); IR (CH_2Cl_2, v_{max} cm^{-1}): 2914, 1602, 1507, 1438, 1380, 1260, 1217, 1164, 1031; R_f = 0.31 EtOAc/hexane (5:95); HRMS (APCI-TOF) (*m/z*) calcd for $C_{10}H_{13}{}^{79}BrO_2S$: 275.9820; found: 275.9841

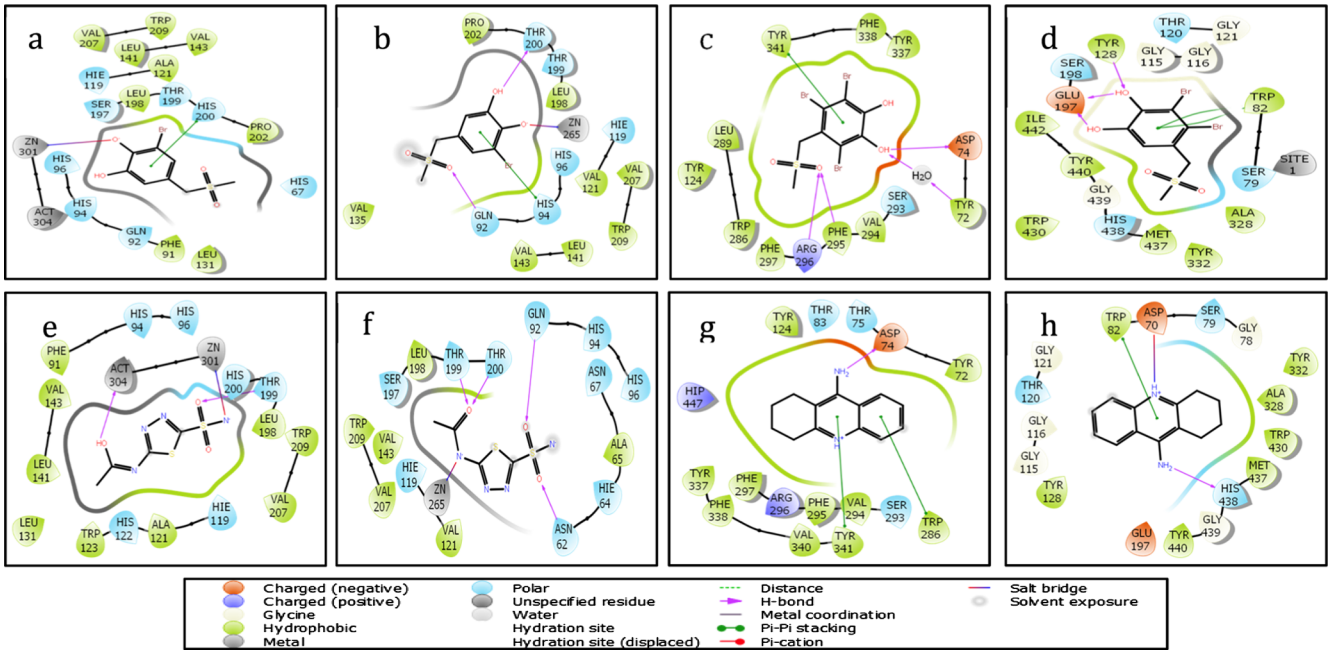

Fig. 5. 2D receptor-ligand interaction profile; (a) 21-hCA I, (b) 21-hCA II, (c) 3-AChE, (d) 2-BChE, (e) AZA-hCA I, (f) AZA-hCA II, (g) TAC-AChE, and (h) TAC-BChE.

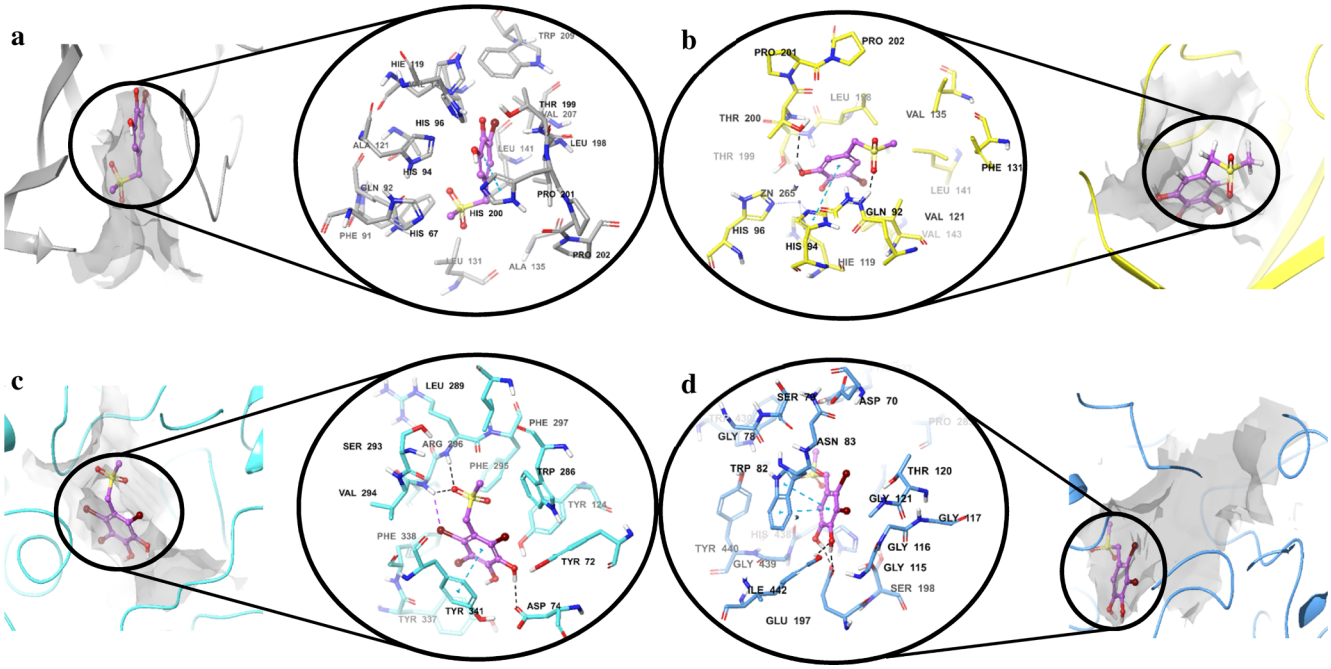

Fig. 6. Superimposed pose of the most active compounds into hCA I, hCA II, AChE, and BChE receptors. (a) Best-pose of 21 into catalytic active site of hCA I, (b) Best-pose of 21 into catalytic active site of hCA II, (c) Best-pose of 3 into catalytic active site of AChE, and (d) Best-pose of 2 into catalytic active site of BChE. Receptors are depicted in the ribbon model which hCA I with grey color, hCA II with yellow color, AChE with cyan color, and BChE with faded blue color. Catalytic active sites are represented as grey solid surface. Compounds are represented in ball and stick modeling which magenta color carbon and residues are represented in thick tube modeling same color with receptors ribbon model.

*4.2.5. Synthesis of 1,2,4-tribromo-5,6-dimethoxy−3-((methylsulfonyl) methyl)benzene (**12**): Standard procedure for the oxidation reaction with m-CPBA*

To a solution of the sulfane **8** (0.3 g, 689.71 μmol) in CH_2Cl_2 (20 mL) was added *m*-CPBA (0.417 g, 2.41 mmol) and $NaHCO_3$ (100 mg) at RT. The reaction mixture was stirred for 24 h at room temperature, and then the reaction mixture was stopped. After a solution of cold $NaHCO_3$ (%5, 0 °C, 100 mL) was slowly added, the mixture was extracted with CH_2CI_2 (2 × 30 mL). Combined organic phases were dried over Na_2SO_4, and the solvent was removed under vacuum. The residue was submitted to silica gel (20 g) column chromatography with EtOAc/hexane (5/95) elution. The sulfone **12** (0.26 g, 81%) was obtained as a white solid. Mp: 98–100 °C; ^{1}H NMR (400 MHz, $CDCl_3$): 5.02 (s, CH_2, 2H), 3.94 (s, OMe, 3H), 3.91 (s, OMe, 3H), 3.04 (s, CH_3, 3H); ^{13}C NMR (100 MHz, $CDCl_3$): 152.67 (C), 151.12 (C), 126.78 (C), 124.21 (C), 122.64 (C), 122.25 (C), 63.25 (CH_2), 60.97 (OMe), 60.93 (OMe), 43.19 (CH_3); IR (CH_2Cl_2, v_{max} cm^{-1}): 2939, 1454, 1393, 1368, 1312, 1285, 1121, 1052, 1007; HRMS (APCI-TOF) calcd for $[C_{10}H_{11}{}^{79}Br_3O_4S + H]^+$: *m/z* = 464.8006; found: 464.8020.

*4.2.6. Synthesis of 3,4,6-tribromo-5-((methylthio)methyl)-1,2-phenylene diacetate (**13**): Standard procedure for the demethylation and acetylation reactions of sulfanes, respectively*

To a stirred solution of the sulfane **8** (0.30 g, 689.71 μmol) in CH_2Cl_2 (15 mL) under nitrogen atmosphere added BBr_3 (380.13 mg, 1.52 mmol) with the aid of a syringe, and the reaction mixture was allowed to stir at RT for 24 h. After the reaction mixture was cooled at 0 °C by ice-water bath, and then MeOH (5 mL) was added dropwise, the solvent was removed under vacuum, and water (5 mL) was added. The reaction mixture was extracted with EtOAc (2 × 15 mL), the combined extracts were dried over Na_2SO_4. The solvent was removed under vacuum. The crude product of the corresponding diol was reacted with Et_3N (2.0 mL) and Ac_2O (2.0 mL) at RT for 24 h, and then CH_2Cl_2 (40 mL) was added. After the reaction mixture was cooled to 0 °C and neutralized by cold solution (%1.0) of HCl. Organic phase was separated and washed by cold solution (%1.0 20 mL) of NaOH and water (20 mL), respectively. After the organic phase was dried over Na_2SO_4, the solvent was removed under vacuum, and diacetate **13** (280 mg 92%) was obtained as a white solid. M.p = 85–87 °C; ^{1}H NMR (400 MHz, $CDCl_3$): 4.23 (s, CH_2S, 2H), 2.35 (s, 2 × $COCH_3$, 6H), 2.21 (s, CH_3S, 3H). ^{13}C NMR (100 MHz, $CDCl_3$): 166.78 (CO), 166.76 (CO), 141.61 (C), 141.58 (C), 138.57 (C), 125.46 (C), 121.76 (C), 119.73 (C), 40.86 (CH_2S), 20.39 (CH_3), 20.35 (CH_3), 16.08 (CH_3S); IR (CH_2Cl_2, v_{max} cm^{-1}): 2917, 2918, 1783, 1412, 1370, 1275, 1189, 1148, 1033, 1011; Rf = 0.43 EtOAc/Hexane (15:85); HRMS (APCI-TOF) (*m/z* + H – 2 CH_3CO - CH_3S) calcd for $C_7H_4{}^{79}Br_2{}^{81}BrO_2$: 358.7741; found: 358.7729.

*4.2.7. Synthesis of 3-bromo-5-((methylthio)methyl)-1,2-phenylene diacetate (**14**)*

This reaction was performed according to the standard procedure described in Section 4.2.6. In the reaction, sulfane **9** (0.50 g, 1.80 mmol), BBr_3 (903.84 mg, 3.61 mmol), Et_3N (2.0 mL), Ac_2O (2.0 mL)) and CH_2Cl_2 (15 mL) were used. Diacetate **14** (0.59 g, 89%) was obtained as a white solid. M.p = 60–62 °C; ^{1}H NMR (400 MHz, $CDCl_3$): 7.44 (s, aromatic, 1H), 7.14 (s, aromatic, 1H), 3.61 (s, CH_2, 2H), 2.33 (s, OAc, 3H), 2.27 (s, OAc, 3H), 2.00 (s, CH_3, 3H); ^{13}C NMR (100 MHz, $CDCl_3$): 167.91 (CO), 167.27 (CO), 143.39 (C), 139.47 (C), 138.24 (C), 130.40 (CH), 123.12 (CH), 117.25 (C), 37.31 (CH_2), 20.60 (CH_3), 20.31 (CH_3), 15.04 (SCH_3); IR (CH_2Cl_2, v_{max} cm^{-1}): 2917, 1779, 1574, 1475, 1371, 1278, 1202, 1015; Rf = 0.37 EtOAc/Hexane (15:85); HRMS (APCI-TOF) (*m/z* + H) calcd for $C_{12}H_{13}{}^{79}BrO_4S$: 332.9796; found: 332.9625.

*4.2.8. Synthesis of 3,4-dibromo-5-((methylthio)methyl)-1,2-phenylene diacetate (**15**)*

This reaction was performed according to the standard procedure described in Section 4.2.6. In the reaction, sulfane **10** (1.0 g, 2.81 mmol), BBr_3 (1.41 g, 5.62 mmol), Et_3N (2.0 mL), Ac_2O (2.0 mL) and CH_2Cl_2 (15 mL) were used. Diacetate **15** (0.93 g, 90%) was

obtained as a white solid. M.p: 82–84 °C; ^{1}H NMR (400 MHz, $CDCl_3$): 7.20 (s, aromatic, 1H), 3.75 (s, CH_2, 2H), 2.26 (s, CH_3, 3H), 2.19 (s, CH_3, 3H), 1.98 (s, SCH_3, 3H); ^{13}C NMR (100 MHz, $CDCl_3$): 167.69 (CO), 167.02 (CO), 142.21 (C), 140.47 (C), 137.80 (C), 124.34 (C), 123.79 (CH), 122.19 (C), 40.05 (CH_2), 20.60 (CH_3), 20.36 (CH_3), 15.35 (SCH_3); IR (CH_2Cl_2, v_{max} cm^{-1}): 2917, 1780, 1446, 1370, 1283, 1196, 1135, 1009; Rf = 0.34 EtOAc/Hexane (15:85); HRMS (APCI-TOF) (*m/z* + H – 2 CH_3CO - CH_3S) calcd for $C_7H_5{}^{79}Br^{81}BrO2$: 280.8636; found: 280.8625.

4.2.9. Synthesis of 4-bromo-5-((methylthio)methyl)-1,2-phenylene diacetate (16)

This reaction was performed according to the standard procedure described in Section 4.2.6. In the reaction, sulfane **11** (0.8 g, 2.89 mmol), BBr_3 (1.45 g, 5.77 mmol), Et_3N (2.0 mL), Ac_2O (2.0 mL) and CH_2Cl_2 (15 mL) were used. Diacetate **16** (0.82 g, 83%) was obtained as a white solid. M.p = 72–74 °C; ^{1}H NMR (400 MHz, $CDCl_3$): 7.42 (s, aromatic, 1H), 7.23 (s, aromatic, 1H), 3.73 (s, CH_2, 2H), 2.26 (s, CH_3, 3H), 2.25 (s, CH_3, 3H), 2.04 (s, SCH_3, 3H); ^{13}C NMR (100 MHz, $CDCl_3$): 168.11 (CO), 168.05 (CO), 141.48 (2 × C), 136.40 (C), 127.91 (CH), 125.16 (CH), 120.73 (C), 38.12 (CH_2), 20.81 (CH_3), 20.75 (CH_3), 15.41 (SCH_3); IR (CH_2Cl_2, v_{max} cm^{-1}): 2917, 1776, 1485, 1370, 1272, 1203, 1133, 1013; Rf = 0.37 EtOAc/Hexane (15:85); HRMS (APCI-TOF) (*m/z* - H) calcd for $C_{12}H_{13}{}^{79}BrO_4S$: 330.9640; found: 330.9635.

4.2.10. Synthesis of 3,4,6-tribromo-5-((methylsulfonyl)methyl)-1,2-phenylene diacetate (17)

This reaction was performed according to the standard procedure described in Section 4.2.5. In the reaction, the diacetate **13** (0.5 g, 1.02 mmol), *m*-CPBA (615.06 mg, 3.56 mmol) and $NaHCO_3$ (100 mg) were used. The sulfone **17** (450 mg, 84%) was obtained as a white solid. M.p = 155–157 °C; ^{1}H NMR (400 MHz, $CDCl_3$): 4.96 (s, CH_2S, 2H), 2.96 (s, CH_3S, 3H), 2.29 (s, 2xCH_3, 6H); ^{13}C NMR (100 MHz, $CDCl_3$): 166.55 (CO), 166.39 (CO), 143.51 (C), 142.21 (C), 129.60 (C), 127.18 (C), 122.67 (C), 121.56 (C), 63.16 (CH_2S), 42.94 (CH_3S), 20.37 (CH_3), 20.31 (CH_3); IR (CH_2Cl_2, v_{max} cm^{-1}): 2931, 1784, 1417, 1372, 1315, 1186, 1148, 1011; HRMS (APCI-TOF) calcd for [$C_{12}H_{11}{}^{79}Br^{81}Br_2O_6S$ + H]: *m/z* = 524.7864; found: 524.7851.

4.2.11. Synthesis of 3-bromo-5-((methylsulfonyl)methyl)-1,2-phenylene diacetate (18)

This reaction was performed according to the standard procedure described in Section 4.2.5. In the reaction, diacetate **14** (1.2 g, 3.60 mmol), *m*-CPBA (2.35 g, 12.61 mmol) and $NaHCO_3$ (100 mg) were used. The sulfone **18** (1.0 g, 76%) was obtained as a white solid. M.p = 128–130 °C; ^{1}H NMR (400 MHz, $CDCl_3$): 7.55 (s, aromatic, 1H), 7.28 (s, aromatic, 1H), 4.18 (s, CH_2, 2H), 2.82 (s, SCH_3, 3H), 2.36 (s, OAc, 3H), 2.29 (s, OAc, 3H); ^{13}C NMR (100 MHz, $CDCl_3$): 167.71 (CO), 166.93 (CO), 143.82 (C), 141.50 (C), 132.13 (CH), 127.84 (C), 124.97 (CH), 118.21 (C), 59.80 (CH_2), 39.44 (SO_2CH_3), 20.59 (CH_3), 20.28 (CH_3); IR (CH_2Cl_2, v_{max} cm^{-1}): 2932, 1776, 1576, 1476, 1425, 1371, 1310, 1200, 1121, 1017; Rf = 0.42 EtOAc/Hexane (6:4); HRMS (APCI-TOF) (*m/z*) calcd for $C_{12}H_{13}{}^{79}BrO_6S$: 363.9616; found: 363.9601.

4.2.12. Synthesis of 3,4-dibromo-5-((methylsulfonyl)methyl)-1,2-phenylene diacetate (19)

This reaction was performed according to the standard procedure described in Section 4.2.5. In the reaction, diacetate **15** (0.5 g, 1.21 mmol), *m*-CPBA (792.38 mg, 4.25 mmol) and $NaHCO_3$ (100 mg) were used. The sulfone **19** (0.43 g, 80%) was obtained as a light yellow solid. M.p = 148–150 °C; ^{1}H NMR (400 MHz, $CDCl_3$): 7.52 (s, aromatic, 1H), 4.59 (s, CH_2, 2H), 2.87 (s, SO_2CH_3, 3H), 2.37 (s, CH_3, 3H), 2.29 (s, CH_3, 3H); ^{13}C NMR (100 MHz, $CDCl_3$): 167.46 (CO), 166.68 (CO), 142.79 (C), 142.54 (C), 128.47 (C), 126.21 (CH), 125.17 (C), 122.79 (C), 61.37 (CH_2), 40.27 (SO_2CH_3), 20.55 (CH_3), 20.34 (CH_3); IR (CH_2Cl_2, v_{max} cm^{-1}): 2917, 2849, 1781, 1450, 1372, 1312, 1195, 1141, 1010; Rf = 0.50 EtOAc/Hexane (6:4); HRMS (APCI-TOF) (*m/z* + H) calcd for $C_{12}H_{12}{}^{79}Br^{81}BrO_6S$: 442.8779; found: 442.8770.

4.2.13. Synthesis of 4-bromo-5-((methylsulfonyl)methyl)-1,2-phenylene diacetate (20)

This reaction was performed according to the standard procedure described in Section 4.2.5. In the reaction, diacetate **16** (0.7 g, 2.10 mmol), *m*-CPBA (1.37 g, 7.35 mmol) and $NaHCO_3$ (100 mg) were used. The sulfone **20** (0.6 g, 78%) was obtained as a white solid. M.p = 145–147 °C; ^{1}H NMR (400 MHz, $CDCl_3$): 7.53 (s, aromatic, 1H), 7.47 (s, aromatic, 1H), 4.46 (s, CH_2, 2H), 2.85 (s, SO_2CH_3, 3H), 2.29 (bs, 2 × CH_3, 6H); ^{13}C NMR (100 MHz, $CDCl_3$): 167.70 (CO), 167.55 (CO), 143.18 (C), 141.80 (C), 128.11 (CH), 127.35 (CH), 126.90 (C), 121.11 (C), 59.55 (CH_2), 39.99 (SO_2CH_3), 20.56 (CH_3), 20.53 (CH_3); IR (CH_2Cl_2, v_{max} cm^{-1}): 2924, 1773, 1490, 1371, 1311, 1204, 1138, 1012; Rf = 0.50 EtOAc/Hexane (6:4); HRMS (APCI-TOF) (*m/z*) calcd for $C_{12}H_{13}{}^{79}BrO_6S$: 363.9616; found: 363.9603.

4.2.14. Synthesis of natural product 3,4,6-tribromo-5-((methylsulfonyl)methyl)benzene-1,2-diol (3): Standard procedure for the synthesis of 2, 21 and 22

A solution of the sulfone **17** (0.2 g, 382.42 μmol) in MeOH (10 mL) was added H_2SO_4 (catalytic), and the mixture was stirred for 6 h at 60 °C. The solvent was removed under vacuum. After H_2O (10 mL) was added to this reaction mixture was added, the mixture was extracted with EtOAc (2 × 10 mL). The combined extracts were dried over Na_2SO_4, the solvent was removed under vacuum and natural product **3** (140 mg, 83%) was obtained as a brown solid. M.p: 195–197 °C [2a] 134–136 °C; ^{1}H NMR (400 MHz, Acetone-d_6): 9.30–8.70 (m, 2 × OH), 4.99 (s, CH_2SO_2, 2H), 3.07 (s, CH_3SO_2, 3H); ^{13}C NMR (100 MHz, Acetone-d_6): 145.24 (C), 143.65 (C), 122.62 (C), 118.87 (C), 114.12 (C), 113.51 (C), 62.82 (CH_2SO_2), 42.70 (CH_3SO_2).

4.2.15. Synthesis of natural product 3-bromo-5-((methylsulfonyl)methyl)benzene-1,2-diol (21)

This reaction was performed according to the standard procedure described in Section 4.2.14. In the reaction, the sulfone **18** (0.3 g, 821.48 μmol), CH_3OH (20 mL)) and H_2SO_4 (catalytic) were used. The bromophenol **21** (0.2 g, 87%) was obtained as a brown solid. M.p = 152–154 °C; ^{1}H NMR (400 MHz, Acetone-d_6): 8.89 (s, OH, 1H), 8.24 (s, OH, 1H), 7.13 (s, aromatic, 1H), 6.97 (s, aromatic, 1H), 4.24 (s, CH_2SO_2, 2H), 2.83 (s, CH_3SO_2, 3H); ^{13}C NMR (100 MHz, Acetone-d_6): 145.95 (C), 143.95 (C), 126.06 (CH), 121.98 (C), 117.16 (CH), 109.26 (C), 59.20 (CH_2SO_2), 38.82 (CH_3SO_2); IR (CH_2Cl_2, v_{max} cm^{-1}): 3412, 2921, 1706, 1588, 1493, 1435, 1293, 1115; Rf = 0.45 MeOH/CH_2Cl_2 (5:95); HRMS (APCI-TOF) (*m/z*) calcd for $C_8H_9{}^{79}BrO_4S$: 279.9405; found: 279.9454.

4.2.16. Synthesis of natural product 3,4-dibromo-5-((methylsulfonyl)methyl)benzene-1,2-diol (2)

This reaction was performed according to the standard procedure described in Section 4.2.14. In the reaction, the sulfone **19** (0.4 g, 900.72 μmol), CH_3OH (20 mL) and H_2SO_4 (catalytic) were used. The natural bromophenol **2** (0.3 g, 92%) was obtained as a cream colored solid. M.p = 188–190 °C; ^{1}H NMR (400 MHz, Acetone-d_6): 9.18 (s, OH, 1H), 8.65 (s, OH, 1H), 7.16 (s, aromatic, 1H), 4.57 (s, CH_2SO_2, 2H), 2.91 (s, CH_3SO_2, 3H); ^{13}C NMR (100 MHz, Acetone-d_6): 146.16 (C), 145.56 (C), 122.36 (C), 118.84 (CH), 118.27 (C), 114.06 (C), 61.66 (CH_2SO_2), 40.59 (CH_3SO_2); Rf = 0.48 MeOH/CH_2Cl_2 (5:95); HRMS (APCI-TOF) (*m/z*) calcd for $C_8H_8{}^{79}Br_2O_4S$: 357.8510; found: 357.8550.

4.2.17. Synthesis of 4-bromo-5-((methylsulfonyl)methyl)benzene-1,2-diol (22)

This reaction was performed according to the standard procedure described in Section 4.2.14. In the reaction, the sulfone **20** (0.45 g, 1.23 mmol), CH_3OH (20 mL) and H_2SO_4 (catalytic) were used. The

bromophenol **22** (0.29 g, 84%) was obtained as a brown solid. M.p = 148–150 °C; ^{1}H NMR (400 MHz, Acetone-d_6): 8.47 (s, OH, 1H), 8.31 (s, OH, 1H), 6.97 (s, aromatic, 1H), 6.95 (s, aromatic, 1H), 4.27 (s, CH_2SO_2, 2H), 2.72 (s, CH_3SO_2, 3H); ^{13}C NMR (100 MHz, Acetone-d_6): 147.80 (C), 145.85 (C), 120.84 (C), 120.09 (2 × CH), 114.69 (C), 60.07 (CH_2SO_2), 40.24 (CH_3SO_2); IR (CH_2Cl_2, v_{max} cm^{-1}): 3259, 2918, 1700, 1512, 1425, 1295, 1138, 1115; Rf = 0.51 MeOH/CH_2Cl_2 (5:95); HRMS (APC-TOF) (*m/z*) calcd for $C_8H_9{}^{79}BrO_4S$: 279.9405; found: 279.9455.

4.3. Biochemical studies

4.3.1. AChE/BChE activity determination and inhibition studies

The inhibitory efficacy of novel benzyl(methyl)sulfane derivative bromophenols (**2, 3, 8–11** and **13–22**) on BChE/AChE activities was obtained conforming to the spectrophotometric procedure of Ellman et al. [37]. Acetylthiocholine iodide (AChI) and butrylcholine iodide (BChI) were used as substrate molecules of the both reactions. In this study, 5,5′-dithio-bis(2-nitro-benzoic)acid (DTNB) was used for the estimation of the both BChE/AChE enzymes activities [38]. Briefly, 100 μL of buffer solution (pH 8.0, 1.0 M, Tris/HCl) and diverse concentration of sample solutions (30–300 μL) dissolved in deionized water were added to 50 μL of both BChE/AChE enzymes solutions (5.32×10^{-3} EU) [39]. Then the mixture was incubated for 10 min at 20 °C. Finally, 50 μL of DTNB (0.5 mM and 25 mL) of both substrate BChI/AChI were added to incubated mixture. Also, the reaction was initiated by the addition of 50 μL of BChI/AChI. Activities of these enzymes were evaluated spectrophotometrically at a wavelength of 412 nm [40].

4.3.2. hCA isoenzyme purification and inhibition studies

For investigating of inhibitory effects of novel benzyl(methyl)sulfane derivative bromophenols (**2, 3, 8–11** and **13–22**) on hCA isoforms, both hCA isoforms from human erythrocytes were purified via a simple single-step by method Sepharose-4B-L-Tyrosine-sulphanilamide affinity gel chromatography [41]. For this purpose, the human erythrocyte samples were centrifuged at 13000 rpm for 25 min. Then, the solution was filtered to remove precipitate. Both hCA isoenzymes were isolated from the serum, which its pH was adjusted to 8.7 by adding solid Tris [42]. The affinity column was equilibrated by buffer solution (25 mM Tris-HCl/0.1 M Na_2SO_4) at the pH 8.7. The serum was loaded to affinity gel and washed with buffer solution (25 mM Tris-HCl/22 mM Na_2SO_4 at the pH 8.7. The hCA I isoenzyme was eluted by buffer solution (1.0 M NaCl/0.25 M sodium phosphate at the pH 6.3. On the other hand, hCA II isoenzyme was eluted by another buffer solution (0.1 M sodium acetate/0.5 M $NaClO_4$ at the pH 5.6. Both isoenzymes were taken from the column in fractions of 2 mL [43]. All works was realized at 4 °C. The hCA isoenzymes activity were measured by following the change at absorbance a specific (348 nm) of p-nitrophenylacetate (PNA) to p-nitrophenolate ion over a period of 3 min at room temperature (25 °C) using a spectrophotometer (Thermo Scientific, UV–Vis Spectrophotometer) according to the method of Verpoorte et al. [44]. There was 0.4 mL of 0.05 M Tris-SO_4 buffer (pH 7.4), 03 mL of 3 mM PNA, 0.2 mL of H_2O, and 0.1 mL of enzyme solution in a test tube content of this reaction [45]. Esterase activity assays were identified from a series of experiments at three different novel benzyl(methyl)sulfane derivative bromophenols (**2, 3, 8–11** and **13–22**).

4.4. In silico studies

4.4.1. Protein and ligand preparation

The *in silico* study was conducted using the Small Drug Discovery Suites package (Schrödinger 2017-2, LLC, USA). X-Ray crystal structures of hCA I, hCA II, AChE, and BChE, (PDB code: 4WR7, 5AML, 4M0E, and 5NN0, respectively) were obtained from RCSB Protein Data Bank (PDB; http://www.rcsb.org/). The crystal structures of receptors were selected because they possess ligand in catalytic active site and smallest resolution of 1.5 Å, 1.36 Å, 2 Å, and 2.1 Å, respectively. Protein preparation wizard panel was used for repairing and preparing of the crystal structures of receptors. Protein preparation workflow was described in summary. Briefly, bond order and charges were assigned and then missing hydrogen atoms were added to crystal structures. Missing side chains were filled using Prime module of the program. Amino acids were ionized by setting physiological pH with the help of Propka software. Water molecules that were formed less than 3 contacts with the protein or ligand were removed. Finally, energy minimization and geometry optimization have also been performed using OPLC force field. 3D structures of synthesized compounds were produced with Maestro 11.4 by sketching 2D structures. 3D structure of ligands was created using LigPrep module of Schrodinger. In order to obtain correct molecular geometries and protonation state at pH 7.0 ± 2.0, Epik module and OPLS-2005 force field were used [46,47].

4.4.2. ADME analysis

To predict pharmacokinetic properties of most active compounds, ADME analysis was performed with QikProp module in Maestro 11.4. The analysis provides information about absorption, distribution, metabolism, and excretion of the compounds in comparison to a particular molecule's properties with those of 95% of known drugs. Pharmacokinetic properties of prepared most active compounds were predicted by using QikProp calculation. The drug-likeness of the compounds was determined with Lipinski's rule of five (mol_MW, logPo/w, donorHB, and accptHB) [48].

4.4.3. Catalytic site prediction

Prediction of catalytic site of the receptors was carried out SiteMap module in Maestro 11.4. The predicted catalytic site provides to select the target for ligand docking and to evaluate docking hits, by showing how well the poses display proper complementarity to the receptor. Prepared receptor was imported into Maestro in PDB file format. SiteMap was run using the default parameter of top-ranked potential protein binding sites setting. This process was performed for all receptors. After SiteMap process, catalytic site for each receptor was generated and Sitescore and Dscore were calculated. The site with the highest Sitescore was selected as catalytic site and induced fit docking (IFD) process was performed on ligand or residue in the catalytic site [49].

4.4.4. Induced fit docking (IFD)

Molecular docking was carried out to characterize binding affinity and interactions between the most active compounds and receptors. Induced Fit Docking (IFD) module in Maestro 11.4 was used for docking process. Centroid of the residues was generated around the selected ligand or residues in the catalytic site of receptor. After that, side chains were automatically trimmed based on B-factor; closest residues to the ligand were refined within 3.4 Å of ligand pose in prime refinement. In order to identification accuracy of the docking process, docking validation was performed with re-docking procedure by evicting inhibitor complexed in the crystal structure of the receptor, before docking of synthesized compounds. Then, most active compounds and were docked on the receptors by IFD methodology. Following the docking process, the types of interactions and interacted residues for best-scored compound results were analyzed [50].

Conflict of interest

The authors declare no competing financial interest.

Acknowledgments

This study was financed by TÜBİTAK - The Scientific and Technological Research Council of Turkey (Project No.: 113Z702) and realized in Atatürk University, Faculty of Science, Department of Chemistry. We are grateful to both institutes for their supports.

Appendix A. Supplementary material

Supplementary data to this article can be found online at https://doi.org/10.1016/j.bioorg.2018.12.012.

References

[1] (a) G.W. Gribble, Chem. Soc. Rev. 28 (1999) 335–346;
(b) M. Ming Liu, P.E. Hansen, X. Lin, Mar. Drugs. 9 (2011) 1273–1292.

[2] (a) X.J. Duan, X.M. Li, B.G. Wang, J. Nat. Prod. 70 (2007) 1210–1213;
(b) H.T. Balaydin, I. Gulcin, A. Menzek, S. Goksu, E. Sahin, J. Enzyme Inhib. Med. Chem. 25 (2010) 685–695;
(c) K. Li, X.M. Li, J.B. Gloer, B.G. Wang, J. Agric, Food. Chem. 59 (2011) 9916–9921;
(d) Y. Cetinkaya, H. Gocer, I. Gulcin, A. Menzek, Arch. Pharm. 345 (2012) 323–334.

[3] K. Kurata, K. Taniguchii, K. Takashima, I. Hayashi, M. Suzuki, Phytochemistry 45 (1997) 485–487.

[4] (a) H.T. Balaydin, M. Senturk, S. Goksu, A. Menzek, Eur. J. Med. Chem. 54 (2012) 423–428;
(b) H.T. Balaydin, M. Senturk, A. Menzek, Bioorg. Med. Chem. Lett. 22 (2012) 1352–1357;
(c) Y. Cetinkaya, H. Goçer, I. Gulcin, A. Menzek, Arch. Pharm. 347 (2014) 354–359.

[5] (a) C. Bayrak, P. Taslimi, I. Gulcin, A. Menzek, Bioorg. Chem. 72 (2017) 359–366;
(b) M. Rezaei, C. Bayrak, P. Taslimi, I. Gulcin, A. Menzek, Turk J. Chem. 42 (2018) 808–825.

[6] Y. Akbaba, C. Turkes, L. Polat, H. Sogut, E. Sahin, S. Goksu, A. Menzek, S. Beydemir, J. Enzyme Inhib. Med. Chem. 28 (2013) 1073–1079.

[7] H. Nozaki, K. Minohara, I. Miyazaki, H. Kondo, F. Shirane, M. Nakayama, Agric. Biol. Chem. 52 (1988) 3229–3230.

[8] (a) M. Senturk, I. Gulcin, A. Dastan, O.I. Kufrevioglu, C.T. Supuran, Bioorg. Med. Chem. 17 (2009) 3207–3211;
(b) T.A. Coban, S. Beydemir, I. Gulcin, D. Ekinci, A. Innocenti, D. Vullo, C.T. Supuran, Bioorg. Med. Chem. 17 (16) (2009) 5791–5795;
(c) S.B. Ozturk Sarikaya, I. Gulcin, C.T. Supuran, Chem. Biol. Drug. Des. 75 (5) (2010) 515–520;
(d) A. Innocenti, S.B. Ozturk Sarıkaya, I. Gulcin, C.T. Supuran, Bioorg. Med. Chem. 18 (6) (2010) 2159–2164.

[9] (a) M. Senturk, I. Gulcin, S. Beydemir, O.I. Kufrevioglu, C.T. Supuran, Chem. Biol. Drugs Des. 77 (6) (2011) 494–499;
(b) S.B. Ozturk Sarikaya, F. Topal, M. Senturk, I. Gulcin, C.T. Supuran, Bioorg. Med. Chem. Lett. 21 (2011) 4259–4262;
(c) K. Aksu, M. Nar, M. Tanç, D. Vullo, I. Gulcin, S. Goksu, F. Tumer, C.T. Supuran, Bioorg. Med. Chem. 21 (2013) 2925–2931.

[10] (a) B. Yigit, M. Yigit, D. Barut Celepci, Y. Gok, A. Aktas, M. Aygun, P. Taslimi, I. Gulcin, ChemistrySelect 3 (27) (2018) 7976–7982;
(b) I. Gulcin, P. Taslimi, Exp. Opin. Therap. Pat. 28 (7) (2018) 541–549.

[11] (a) M. Guney, A. Coskun, F. Topal, A. Dastan, I. Gulcin, C.T. Supuran, Bioorg. Med. Chem. 22 (2014) 3537–3543;
(b) S. Goksu, A. Naderi, Y. Akbaba, P. Kalın, A. Akincioglu, I. Gulcin, S. Durdagi, R.E. Salmas, Bioorg. Chem. 56 (2014) 75–82.

[12] (a) M. Boztas, Y. Cetinkaya, M. Topal, I. Gulcin, A. Menzek, E. Sahin, M. Tanc, C.T. Supuran, J. Med. Chem. 58 (2) (2015) 640–650;
(b) A. Yıldırım, U. Atmaca, A. Keskin, M. Topal, M. Celik, I. Gulcin, C.T. Supuran, Bioorg. Med. Chem. 23 (2015) 2598–2605.

[13] (a) A. Akincioglu, H. Akincioglu, I. Gulcin, S. Durdagı, C.T. Supuran, S. Goksu, Bioorg. Med. Chem. 23 (13) (2015) 3592–3602;
(b) T. Artunc, Y. Cetinkaya, H. Gocer, I. Gulcin, A. Menzek, E. Sahin, C.T. Supuran, Chem. Biol. Drug Des. 87 (4) (2016) 594–607;
(c) B. Ozgeris, S. Goksu, L. Kose Polat, I. Gulcin, R.E. Salmas, S. Durdagi, F. Tumer, C.T. Supuran, Bioorg. Med. Chem. 24 (10) (2016) 2318–2329.

[14] (a) H. Genc, R. Kalin, Z. Koksal, N. Sadeghian, U.M. Kocyigit, M. Zengin, I. Gulcin, H. Ozdemir, Int. J. Mol. Sci. 17 (2016) 1736;
(b) F. Topal, I. Gulcin, A. Dastan, M. Guney, Int. J. Biol. Macromol. 94 (2017) 845–851;
(c) H. Gocer, A. Akincioglu, S. Goksu, I. Gulcin, Arab. J. Chem. 10 (3) (2017) 398–402;
(d) U.M. Kocyigit, Y. Budak, M.B. Gurdere, S. Tekin, T. Kul Koprulu, F. Erturk, K. Ozcan, I. Gulcin, M. Ceylan, Bioorg. Chem. 70 (2017) 118–125.

[15] H.I. Gul, A. Demirtas, G. Ucar, P. Taslimi, I. Gulcin, Lett. Drug Des. Discov. 14 (5) (2017) 573–580.

[16] (a) A. Aktas, P. Taslimi, I. Gulcin, Y. Gok, Arch. Pharm. 350 (6) (2017) e1700045;
(b) N. Oztaskın, P. Taslimi, A. Maras, S. Goksu, I. Gulcin, Bioorg. Chem. 74 (2017) 104–114;
(c) A. Akincioglu, E. Kocaman, H. Akıncıoglu, R.E. Salmas, S. Durdagı, I. Gulcin, C.T. Supuran, S. Goksu, Bioorg. Chem. 74 (2017) 238–250.

[17] (a) I. Gulcin, M. Abbasova, P. Taslimi, Z. Huyut, L. Safarova, A. Sujayev, V. Farzaliyev, S. Beydemir, S.H. Alwasel, C.T. Supuran, J. Enzyme Inhib. Med. Chem. 32 (1) (2017) 1174–1182;
(b) U.M. Kocyigit, Y. Budak, F. Eliguzel, P. Taslimi, D. Kılıc, I. Gulcin, M. Ceylan, Arch. Pharm. 350 (12) (2017) e1700198;
(c) U.M. Kocyigit, Y. Budak, M.B. Gurdere, F. Erturk, B. Yencilek, P. Taslimi, I. Gulcin, M. Ceylan, Synthet. Commun. 47 (24) (2017) 2313–2323;
(d) P. Taslimi, C. Caglayan, I. Gulcin, J. Biochem. Mol. Toxicol. 31 (12) (2017) e21995.

[18] (a) F. Erdemir, D. Barut Celepci, A. Aktas, P. Taslimi, Y. Gok, H. Karabiyik, I. Gulcin, J. Mol. Struct. 1155 (2018) 797–806;
(b) S. Burmaoglu, A.O. Yilmaz, P. Taslimi, O. Algul, D. Kılıc, I. Gulcin, Arch. Pharm 351 (2) (2018).

[19] H.L. Holland, F.M. Brown, B.G. Larsen, Tetrahedron-Asymmetry. 6 (1995) 1561–1567.

[20] (a) A.A. Kaya, A. Menzek, E. Sahin, Tetrahedron. 70 (2014) 83–91;
(b) W.J.N. Meester, J.H. Van Maarseveen, K. Kirchsteiger, P.H.H. Hermkens, H.E. Schoemaker, H. Hiemstra, F.P.J.T. Rutjes, Arkivoc (2004) 122–151.

[21] (a) T. Mori, H. Bando, Y. Kanaiwa, T. Amiya, K. Kurata, Chem. Pharm. Bull. 31 (1983) 1754–1756;
(b) Y. Akbaba, H.T. Balaydin, S. Goksu, E. Sahin, A. Menzek, Helv. Chim. Acta. 93 (2010) 1127–1135;
(c) H.T. Balaydin, Y. Akbaba, A. Menzek, E. Sahin, S. Goksu, Arkivoc XIV (2009) 75–87.

[22] (a) T.M. Kosak, H.A. Conrad, L. Andrew, A.L. Korich, R.L. Lord, Eur. J. Org. Chem. (2015) 7460–7467;
(b) Y. Akbaba, H.T. Balaydin, A. Menzek, S. Goksu, E. Sahin, D. Ekinci, Arch. Pharm. 346 (2013) 447–454.

[23] (a) H.T. Balaydin, J. Chem. Res. (2012) 238–240;
(b) A.A. Kaya, M.E. Sengul, A. Menzek, I. Kayaardi, M. Karakus, E. Sahin, J. Chem. Res. (2011) 540–544;
(c) A. Menzek, M. Balci, Tetrahedron 49 (1993) 6071–14078.

[24] (a) U.M. Kocyigit, Y. Budak, M.B. Gurdere, F. Erturk, B. Yencilek, P. Taslimi, I. Gulcin, M. Ceylan, Arch. Physiol. Biochem. 124 (1) (2018) 61–68;
(b) C. Yamali, H.I. Gul, A. Ece, P. Taslimi, I. Gulcin, Chem. Biol. Drug Des. 91 (4) (2018) 854–866.

[25] (a) P. Taslimi, I. Gulcin, J. Food Biochem. 42 (3) (2018) e12516;
(b) P. Taslimi, İ. Gulcin, B. Ozgeris, S. Goksu, F. Tumer, S.H. Alwasel, C.T. Supuran, J. Enzyme Inhib. Med. Chem. 31 (2016) 152–157.

[26] (a) H.I. Gul, K. Kucukoglu, C. Yamali, S. Bilginer, H. Yuca, I. Ozturk, P. Taslimi, I. Gulcin, C.T. Supuran, J. Enzyme Inhib. Med. Chem. 31 (4) (2016) 568–573;
(b) M. Kucuk, I. Gulcin, Environ. Toxicol. Pharmacol. 44 (2016) 134–139.

[27] (a) P. Taslimi, I. Gulcin, N. Oztaskin, Y. Cetinkaya, S. Goksu, S.H. Alwasel, C.T. Supuran, J. Enzyme Inhib. Med. Chem. 31 (4) (2016) 603–607;
(b) D. Ozmen Ozgun, C. Yamali, H.I. Gul, P. Taslimi, I. Gulcin, T. Yanik, C.T. Supuran, J. Enzyme Inhib. Med. Chem. 31 (6) (2016) 1498–1501.

[28] A. Sujayev, E. Garibov, P. Taslimi, I. Gulcin, S. Gojayeva, V. Farzaliyev, S.H. Alwasel, C.T. Supuran, J. Enzyme Inhib. Med. Chem. 31 (6) (2016) 1531–1539.

[29] (a) H.I. Gul, M. Tugrak, H. Sakagami, P. Taslimi, I. Gulcin, C.T. Supuran, J. Enzyme Inhib. Med. Chem. 31 (6) (2016) 1619–1624;
(b) R. Kocak, E. Turan Akin, P. Kalin, O. Talaz, N. Saracoglu, A. Dastan, I. Gulcin, S. Durdagi, J. Heterocyc. Chem. 53 (6) (2016) 2049–2056.

[30] (a) B. Turan, K. Sendil, E. Sengul, M.S. Gultekin, P. Taslimi, I. Gulcin, C.T. Supuran, J. Enzyme Inhib. Med. Chem. 31 (S1) (2016) 79–88;
(b) F. Ozbey, P. Taslimi, I. Gulcin, A. Maras, S. Goksu, C.T. Supuran, J. Enzyme Inhib. Med. Chem. 31 (S2) (2016) 79–85.

[31] (a) E. Garibov, P. Taslimi, A. Sujayev, Z. Bingol, S. Cetinkaya, I. Gulcin, S. Beydemir, V. Farzaliyev, S.H. Alwasel, C.T. Supuran, J. Enzyme Inhib. Med. Chem. 31 (S3) (2016) 1–9;
(b) K. Aksu, B. Ozgeris, P. Taslimi, A. Naderi, I. Gulcin, S. Goksu, Arch. Pharm. 349 (12) (2016) 944–954;
(c) M. Isik, S. Beydemir, A. Yılmaz, M.E. Naldan, H.E. Aslan, I. Gulcin, Biomed. Pharmacother. 87 (2017) 561–567.

[32] P. Taslimi, A. Sujayev, S. Mamedova, P. Kalin, I. Gulcin, N. Sadeghian, S. Beydemir, O.I. Kufrevioglu, S.H. Alwasel, V. Farzaliyev, S. Mamedov, J. Enzyme Inhib. Med. Chem. 32 (1) (2017) 137–145.

[33] (a) H. Akincioglu, I. Gulcin, S.H. Alwasel, Fresen. Environ. Bull. 26 (6) (2017) 3733–3739;
(b) L. Polat Kose, I. Gulcin, Rec. Nat. Prod. 11 (6) (2017) 558–561.

[34] (a) P. Taslimi, A. Sujayev, E. Garibov, N. Nazarov, Z. Huyut, S.H. Alwasel, I. Gulcin, J. Biochem. Mol. Toxicol. 31 (7) (2017) e21897;
(b) P. Taslimi, S. Osmanova, I. Gulcin, S. Sardarova, V. Farzaliyev, A. Sujayev, R. Kaya, F. Koc, S. Beydemir, S.H. Alwasel, O.I. Kufrevioglu, J. Biochem. Mol. Toxicol. 4 31 (9) (2017) e21931.

[35] C.A. Lipinski, F. Lombardo, B.W. Dominy, P.J. Feeney, Adv. Drug Deliv. Rev. 23 (1997) 3–25.

[36] H. Senol, C. Bayrak, A. Menzek, E. Sahin, M. Karakus, Tetrahedron. 72 (2016) 2587–2592.

[37] G.L. Ellman, K.D. Courtney, V. Andres, R.M. Featherston, Biochem. Pharmacol. 7 (1961) 88–95.

[38] U.M. Kocyigit, P. Taslimi, H. Gezegen, I. Gulcin, M. Ceylan, J. Biochem. Mol. Toxicol. 31 (9) (2017) e21938.

[39] T. Dastan, U.M. Kocyigit, S.D. Dastan, C. Kilickaya, P. Taslimi, C. Ozge, M. Koparir, A. Cetin, C. Orek, I. Gulcin, J. Biochem. Mol. Toxicol. 31 (11) (2017) e21971.

[40] P. Taslimi, H. Akincioglu, I. Gulcin, J. Biochem. Mol. Toxicol. 31 (11) (2017) e21973.

[41] U.M. Kocyigit, A. Taskiran, P. Taslimi, A. Yokus, Y. Temel, I. Gulcin, J. Biochem. Mol. Toxicol. 31 (11) (2017) e21972.

[42] U.M. Kocyigit, S. Durna Dastan, P. Taslimi, T. Dastan, I. Gulcin, J. Biochem. Mol. Toxicol. 32 (1) (2018) e22000.

[43] N. Bulut, U.M. Kocyigit, I.H. Gecibesler, T. Dastan, H. Karci, P. Taslimi, S. Durna Dastan, I. Gulcin, A. Cetin, J. Biochem. Mol. Toxicol. 32 (1) (2018) e22006.

[44] J.A. Verpoorte, S. Mehta, J.T. Edsall, J. Biol. Chem. 242 (1967) 4221–4229.

[45] (a) Y. Sari, A. Aktas, P. Taslimi, Y. Gok, C. Caglayan, I. Gulcin, J. Biochem. Mol. Toxicol. 32 (1) (2018) e22009;
(b) C. Caglayan, I. Gulcin, J. Biochem. Mol. Toxicol. 32 (1) (2018) e22010.
[46] Drug Discovery Suite, Schrödinger, LLC, New York, NY, 2017.
[47] B. Yigit, R. Kaya, P. Taslimi, Y. Isik, M. Karaman, M. Yigit, I. Ozdemir, I. Gulcin, J. Mol. Struct. 1179 (2018) 709–718.
[48] QikProp, version 4.4, Schrödinger, LLC, New York, NY, 2015.
[49] SiteMap, version 2.3, Schrödinger, LLC, New York, NY, 2009.
[50] Schrödinger Suite 2009 Induced Fit Docking protocol; Glide version 5.5, Schrödinger, LLC, New York, NY, 2009; Prime version 2.1, Schrödinger, LLC, New York, NY, 2009.